Int. J. of Thermal & Environmental Engineering
Volume 20, No. 1 (2023) 35-39

Analysis and Sensitivity Studies on Thermoacoustic Engine Stack Temperature Profile Development

Timileyin Aworinde, Alfiya Simran, Isam Janajreh*

Mechanical Engineering Department, Khalifa University of Science and Technology, Abu Dhabi, United Arab Emirates

Abstract

Thermoacoustic engines are devices that convert thermal energy to acoustic energy using the Stirling cycle principle. They have wide importance in refrigeration and power generation, therefore there has been intensified research in this area. High focus has particularly been on exploring ways to improve the efficiency of the thermoacoustic engine, the non-linearity of the temperature profile developed across the stack of the engine poses a hindrance to the efficiency of the engine because the thermal gradient across the stack greatly affects the performance of the engine. This work therefore investigates possible pathways for improving the linearity of the temperature gradient across the stack. Two methods of heating the engines are investigated, namely top heating and side heating. For the former the heat is supplied externally at the top of the resonator while in the latter is done internally at the sides of the stack. Different stack materials and fluid medium are also varied to observe their influence on the temperature gradient across the stack. The results of the conducted analysis show that the internal heating condition has a higher tendency to produce a linear temperature gradient across the stack compared to the top heating. The variation of stack materials shows that the linearity of the temperature gradient of the stack increases with the thermal conductivity of the stack materials as materials with very high thermal conductivities (e.g., diamond) produced a perfectly linear temperature gradient across the stack. For the fluid medium, it is also seen that the linearity of the temperature gradient across the stack improves with increase in specific heat and thermal conductivity of the fluid medium with helium giving the most linear gradient of all the medium investigated.

Keywords: *Thermoacoustic engine; thermoacoustic refrigerator; stack heating; stack materials; CFD*

1. Introduction

Thermoacoustics can be referred to as the interaction between pressure, temperature, and density variation of acoustic waves [1]-[4]. An important application of this phenomenon is in the thermoacoustic engine. The thermoacoustic engine (TAE) is a device that produces work from heat and energy in the form of acoustic energy. To generate the acoustic energy, a thermal gradient must be developed in the stack of the TAE. The stack is an important component of the TAE, and it is simply a porous solid component that allows working gas fluid to oscillate within the boundaries of the TAE [5]-[7]. These engines are known for their simple, efficient, and reliable design. They utilize inert gases as the working fluid and possess no moving parts which makes it possible to produce mechanical energy sustainably. These engines are commonly applied in the field of refrigeration where the cooling effect is produced by utilizing acoustic power to pump heat from the source to the sink. The two basic types of thermoacoustic engines usually studied are the standing and moving/traveling wave thermoacoustic engines [1].

In literature, several works have been done on the experimental and numerical design of thermoacoustic engines; Ali et al. [8], [9] worked on the numerical simulation and experimental validation of the Thermoacoustic engine. According to the study, the engine's performance was affected by the stack length and location within the resonator tube. It was experimentally validated that the efficiency of

* Corresponding author. Tel.: +971 2 312 3286
E-mail: Isam.Janajreh@ku.ac.ae

DOI: 10.5383/ijtee.20.01.006

the engine increased as the center position of the stack moved further away from the pressure anti node. Additionally, the study's conclusion discussed the impact of engine efficiency on stack length, concluding that the longer the stack, the better the engine performance. Following this principle, Hariharan et al. [10] studied the effect of stack geometry and resonator length on the performance of thermoacoustic engines. In the study, theoretical and experimental investigations were carried out to examine the influence of plate thickness, plate spacing, and resonator length with constant stack length on the performance of standing wave thermoacoustic prime mover. The system performance was observed in terms of temperature difference, frequency, and pressure amplitude. The results of the study showed that an increase in the plate spacing, and resonator length leads to a decrease in working frequency, it however leads to an increase in both onset temperature difference and pressure amplitude for the plates. Conclusively, the acoustic power decreased with an increase in resonator length and a decrease in plate thickness. Yu et al. [11] developed a CFD simulation for an experimental 300Hz standing wave thermoacoustic heat engine. The results showed that a porous media model was not suitable for the stack simulation, rather a fluid-solid coupled model gave appropriate results. Through the analysis, it was found that there is no Gedeon DC flow existing in the standing wave engine, which validates the simulation. Additionally, nonlinear vortex evolution in the ends of the stack and the gas reservoir of the resonator is shown as earlier described in other studies. The numerical model was further seen to have good agreement with the experimental results. Another work in this field was done by Elshabrawy et al. [12], where a numerical study of a standing wave thermoacoustic engine was carried out in order to investigate the pressure variations over time in the resonator tube and to analyze the thermoacoustic performance of the engine. The results obtained in this study denotes the changes in pressure at specified locations and the emergence of temperature profiles inside the resonator. The study also deals with the effect of different working fluids and their thermal properties on the pressure wave developed in thermoacoustic engine. Gas mixtures of CO_2 – air, and Helium – air with varying compositions were considered in this work. It was noticed that in the Helium-air mixture the onset of the pressure wave was quicker than in only air or CO_2 compositions, while there was no pressure wave development in the Helium-only composition. The study was concluded by showing the importance of the thermal properties of the working fluid to the pressure wave. Dong et al. [13] also investigated the effect of different types of working fluids on the performance of thermoacoustic engines. Temperature, frequency, and pressure of working fluids like helium, argon, and nitrogen were used as analysis parameters in this work. The results of the study showed that an optimum value of mean pressure (0.7 – 1.0 MPa) appears when the TAE is filled with helium alone, however, nitrogen and argon were noticed to work in higher pressure ranges as compared to helium. Conclusively, the working frequency of helium was seen to be approximately 3 times of the two other gases irrespective of the working conditions. Zhang et al. [14] developed a numerical simulation for a travelling wave thermoacoustic engine, in their work, the effects of working fluid, heating source, resonator geometry and configuration on the pressure level and frequency of the generated acoustic wave were investigated. The work done showed that frequency and pressure waves increase with increase in the temperature. For the fluid behavior, it was seen that air and nitrogen resulted in similar acoustic wave generation. Meanwhile, the acoustic wave that was generated by helium produced a higher frequency than nitrogen but with a lower pressure level. It was concluded that longer stack lengths led to similar wave forms.

Earlier research done in the analysis of standing wave thermoacoustic engine have analyzed the whole length of the thermoacoustic engine, for the stack temperature profile, a linear temperature profile was imposed on the stack. For numerical simulations, the imposition of linear temperature profile on the stack gives high efficiency values for the engine, however this cannot be replicated experimentally as the linear profile imposition is not feasible physically, and the experimental procedure therefore gives very low efficiency values for the engine. To investigate numerically ways in which better efficiency can be obtained without the imposition of linear temperature, this work therefore aims to analyze scenarios in which the optimum linear temperature profile can be obtained across the stack.

This project focuses on a smaller section of the TAE with more emphasis on the stack and the analysis of the temperature profile across it. This work investigates the sensitivity analysis of a standing wave thermoacoustic engine section to determine the effect of different parameters on the temperature gradient across the stack in the engine. This study proposes to investigate the effect of varying stack materials (steel, copper, diamond, brass and nickel), velocity/pressure boundary conditions and working fluid (Air, Helium, Argon, methane and CO_2) on the temperature gradient across the stack. The methodology being proposed is to develop a two-dimensional computational fluid dynamics model using Ansys Fluent software, the model developed will be analyzed to verify the effects of the above-listed parameters on the conjugated heating across the stack in the engine.

2. Methodology

For this work, a thermoacoustic engine is modeled within Ansys/Fluent with the geometry designed to be axisymmetric. The engine consists of horizontal plates of stack within the resonator tube. The horizontal plates in the stack have thicknesses of 5mm and the space between each plate is 2mm. These lengths are considered based on previous analysis by the author that produces the oscillating acoustic pressure wave. The resonator tube is open-ended at one side and is closed at other end, and it has a reduced length of 43.8cm and a radius of 3.655cm. A high-resolution mesh for the work was created in Gambit for the geometry. The different types of mesh explored in this work are described in Table 1 of the results section. The geometry of the base model mesh is shown in Figure 1. The flow in the setup is to be steady, non-isothermal and two-dimensional Navier-stokes. The turbulence of the model is aptly represented

by the k-ε turbulence model. The governing equation for the system model is described in the subsequent equations.

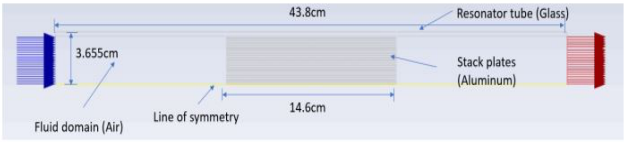

Fig. 1. Schematic of TAE

The expression for the conservation of mass in axisymmetric geometry is shown in equation 1.

$$\frac{\partial(\rho_f)}{\partial t} + \frac{1}{r}\frac{\partial(r\rho_f v_f)}{\partial r} + \frac{\partial(\rho_f v_x)}{\partial x} \quad (1)$$

where, v, ρ, x, r, f subscript, and t subscript represent the velocity, density, axial coordinates, radial coordinates, fluid and time respectively.

The expression for the conservation of momentum is shown in equation 2.

$$\frac{\partial(\rho_f \bar{v})}{\partial t} + \nabla.\left(\rho_f \bar{v}\bar{v}\right) = -\nabla p + \nabla.(\tau) \quad (2)$$

where, τ and p represents stress tensor and pressure, respectively.

The expression for the conservation of energy in the fluid flow is represented as equation 3.

$$\frac{\partial(\rho_f E)}{\partial t} + \nabla.\left(\vec{v}\left(\rho_f E + p\right)\right) = \nabla.[\hat{k}\nabla T + (\tau.\vec{v})] \quad (3)$$

where, T, E and k represent the temperature, internal energy and thermal conductivity respectively.

The Ideal gas law is shown in equation 4.

$$p = \rho RT \quad (4)$$

where, R is the gas constant.

The expression for the conservation of energy of the solid area of the stack is given as equation 5.

$$\rho_s C_s \frac{dT_s}{dt} = \nabla.(K\nabla T_s) \quad (5)$$

where, the heat capacity is represented by C and s subscript stands for solid.

All walls except the outlet are assigned the no-slip boundary condition. The left end of the TAE stack is heated at 1000K temperature, while the cold end of the stack is kept at 300K. The temperature gradient across the stack is allowed to develop through conjugated heating. A constant velocity of 1m/s was applied at the entry of the resonator and gauge pressure of zero is kept at the outlet boundary condition.

The analysis in this work is the sensitivity study that aims to analyze the variation of the temperature gradient across the stack with different heat addition methods, material types, fluid medium, inlet velocity/pressure boundary conditions. For the heating methods top and side (internal) heat are considered in this work. In top heating, the hot and cold temperatures are fixed on top of the resonator tube, the heating area is varied from 5% to 15% with an increment of 5. In the side heating however, the hot temperature was fixed at the left side of the stack internally and the cold at the right side of the stack. Different analyses were carried on the individual conditions.

For material analysis, steel, copper, diamond, brass and nickel were used, also for the fluid medium investigated, Air, Helium, CO_2 and Argon were investigated, and the temperature gradient was recorded with the different parameters. A comparative analysis of the effects of the varying parameter on the temperature across the stack is done and compared as seen in the following section.

3. Results and discussion

In this work, four mesh types—Fine, Baseline, Coarse 1 and Coarse 2—were created to evaluate the solution independence. Table 1 illustrates the characteristics of each mesh type. Based on the heat transfer to the stack and the average temperature distribution across the stack, the mesh correlations were examined. The baseline mesh with 142,000 cell counts is chosen for further research in this work because it was determined that the disparity from the fine mesh was within acceptable bounds.

Table 1: Mesh sensitivity results

Mesh	Cells Count	Heat transfer rate (W) (error %)	Average of Temp. (error %)
Fine	285,120	-578.08 (-)	630.74 (-)
Baseline	142,560	-579.23 (0.2 %)	618.25 (2.0 %)
Coarse 2	71,280	-577.88 (0.04 %)	617.57 (2.09 %)
Coarse 1	35,640	-678.73 (17.4 %)	609.73 (3.33 %)

The investigation of top heating is illustrated in Figure 2. The results indicate that most of the heat is dissipated through the glass, which resulted in a nonlinear temperature profile across the stack. Thus, as already demonstrated experimentally, this lowers the efficiency that may be attained in the thermoacoustic engine. Although there is some improvement as the percentage of heating area increases, the effect is not sufficient to give a linear temperature distribution across the stack. Figure 3. shows the comparison of the 5%, 10% and 15% heating and higher temperature limits are obtained in the 15% heating condition as compared to other conditions.

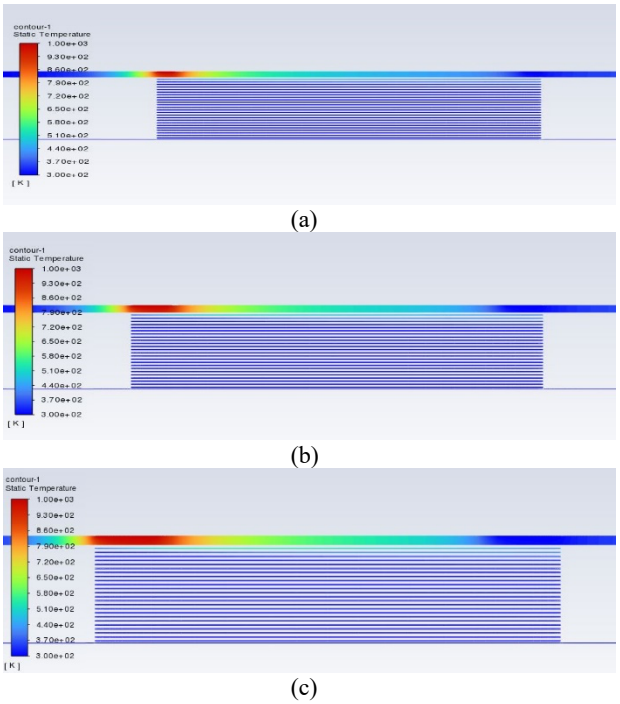

(a)

(b)

(c)

Fig. 2. Top heating temperature distribution results at (a) 5% of stack length (b) 10% of stack length (c) 15% of stack length

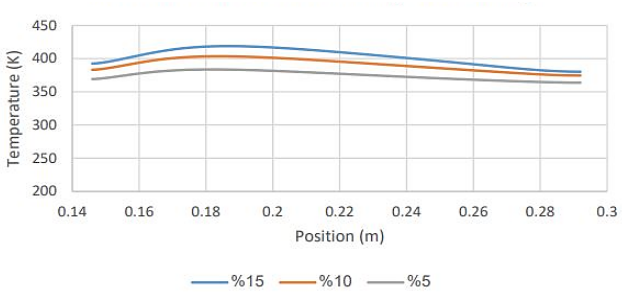

Fig. 3. Comparison of different top area percentages of top heating

Due to the non-linearity observed in the top heating, the side heating of the stack was carried out that is illustrated in the figure. It is observed that the side heating gives more favorable temperature profile across the stack compared to the top heating. As shown in Figure 4, using steel as the stack material and air as the fluid medium, it can be observed that the temperature profile improved in terms of linearity when compared with the top heating. Figure 4 shows that with variation of certain modeling parameters which includes the method of stack heating, it is possible to get a linear profile for the temperature distribution across the stack.

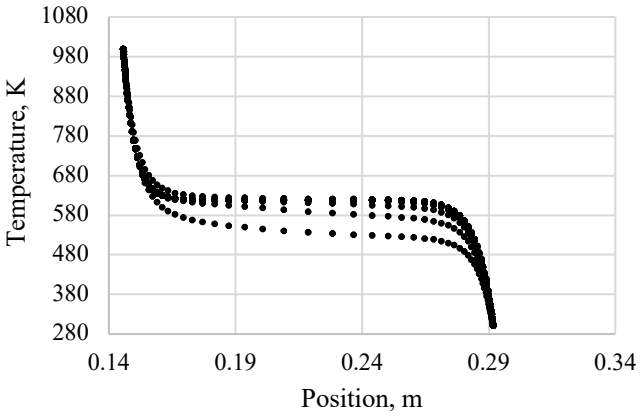

Fig. 4. Stack temperature profile using side heating and steel material

To investigate the possible conditions that could improve the temperature distribution across the stack, different materials of stack are investigated. The properties of different materials are stated in Table 2. From the results obtained in this analysis, brass and copper have an almost linear temperature profile, and diamond, a material with very high thermal conductivity had a perfectly linear temperature profile. We can infer from this analysis that the thermal conductivity of the stack material has an impact on the linearity of the temperature profile across the stack.

Table 2: Properties of stack materials investigated

	Density (Kg/m^3)	Specific heat (J/Kg K)	Thermal Conductivity (W/m K)
Brass	8514	380	122
Copper	7639	392	398
Diamond	3509	529	1445
Nickel	8400	415	67
Steel	8030	503	45

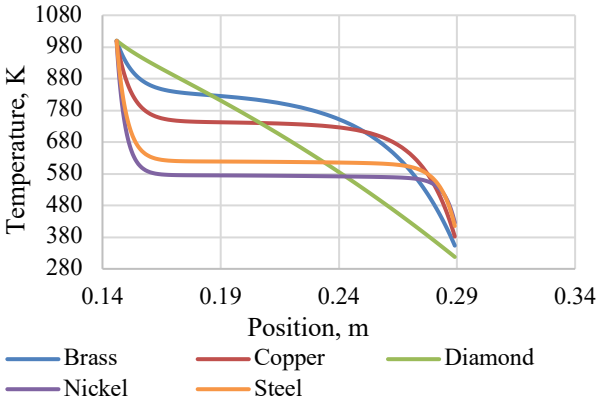

Fig. 5. Temperature profile across stack with different stack materials

The linearity of the temperature profile across the stack were also studied by varying the working fluid in the resonator. However, for the analysis, the material of stack was kept constant as steel. The different fluid materials investigated, and their properties are stated in Table 3. From the results obtained in this work, it is seen that Helium had the most favorable temperature profile across the stack in terms of linearity while CO_2 had the least favorable profile, which is illustrated in Figure 6. It can be inferred from this trend that the linearity of the temperature profile across the stack improves with increase in thermal conductivity and specific heat capacity of the fluid medium.

Table 3: Properties of fluid medium investigated

	Density (Kg/m^3)	Specific heat (J/Kg K)	Thermal Conductivity (W/m K)
Argon	1.6228	520.64	0.0158
CO_2	1.7878	840.37	0.0145
Helium	0.1625	5193	0.152
Methane	0.6679	2222	0.0322
Air	1.225	1006.43	0.0242

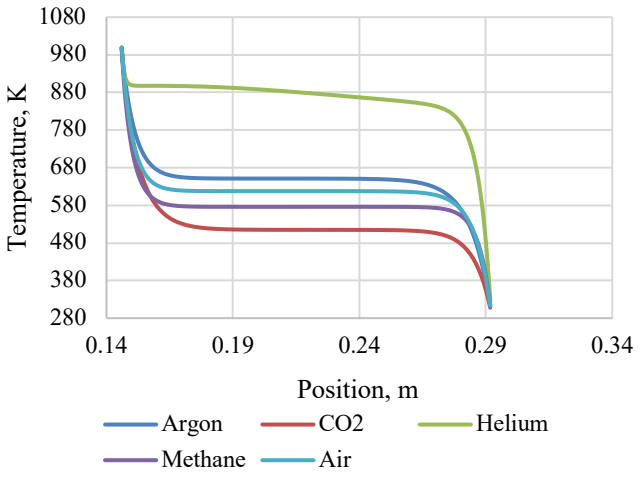

Fig. 6. Temperature profile across stack with different fluid medium

4. Conclusions

In this work, numerical simulations, and analysis on the temperature profile across the stack of a standing wave thermoacoustic engine are carried out. The effects of top heating and internal heating, working fluid, stack material on the temperature profile developed across the stack are studied. The important findings from the work are as follows:

- Four different meshes were developed, namely, Fine, Baseline, Coarse 1 and Coarse 2 of which the mesh sensitivity analysis validated the accuracy of the meshing process.
- Two methods of stack heating; Top heating and Internal heating, were considered and analyzed.
- 5%, 10% and 15% of the top glass surface was heated of which the 15% surface heating gave the highest heat transfer to the stack.
- The temperature profile across the stack developed in top heating was not close to being linear which necessitated internal heating analysis.
- Analysis of stack material with internal heating shows that the linearity of the profile improves with increase in thermal conductivity of the material.
- Analysis of fluid medium with internal heating shows that the linearity of the profile improves with increase in thermal conductivity and specific heat capacity of the fluid.

This research provides the results to get a linear temperature profile across the stack which is an effective design criterion to increase the performance of a standing wave thermoacoustic engine. It provides comparative analysis of different parameters that can help in achieving an optimum linear temperature gradient across the stack of the thermoacoustic engine. To further examine and analyze the standing wave thermoacoustic engine, the following works are recommended for exploration:

- The analysis on the temperature profile developed across the stack could be extended to a transient analysis by imposing fluctuating pressure across the boundary.
- The results of the computational research on the side heating of the stack could be validated experimentally.
- The findings of this study could be used to conduct a performance analysis of the standing wave thermoacoustic engine since they indicate variables that can provide a linear temperature profile across the stack, which can enhance the system's ability to generate acoustic power.

Acknowledgments

We would like to acknowledge Khalifa University of Science and Technology, Abu Dhabi, UAE, for providing the opportunity and support in conducting this work.

References

[1] U. Ali, O. Al-Mufti, and I. Janajreh, "Harnessing sound waves for sustainable energy: Advancements and challenges in thermoacoustic technology," *Energy Nexus*, vol. 15, p. 100320, Sep. 2024, doi: 10.1016/j.nexus.2024.100320.

[2] G. W. Swift and S. L. Garrett, "*Thermoacoustics: A Unifying Perspective for Some Engines and Refrigerators*," *The Journal of the Acoustical Society of America*, vol. 113, no. 5, pp. 2379–2381, May 2003, doi: 10.1121/1.1561492.

[3] U. Ali, H. Zhang, S. Abedrabbo, and I. Janajreh, "Freeze desalination via thermoacoustic cooling: System analysis and cost overview," *Energy Nexus*, vol. 10, p. 100195, Jun. 2023, doi: 10.1016/j.nexus.2023.100195.

[4] I. Janajreh, D. Islam, S. Abedrabbo, H. Zhang, and U. Ali, *Integrated Thermoacoustic Freeze Desalination Systems and Processes*. US Patent WO/2022/175,897, 2022.

[5] U. Ali, S. Abedrabbo, M. Islam, and I. Janajreh, "Numerical Simulation Of Thermoacoustic Refrigerator Coupled With Thermoacoustic Engine," presented at the 15th International Conference On Heat Transfer, Fluid Mechanics And Thermodynamics, Jul. 2021.

[6] O. A. Al-Mufti and I. Janajreh, "Thermoacoustic Refrigeration: Short Review," *Int. J. of Thermal & Environmental Engineering*, vol. 19, no. 1, pp. 29–45, 2022, doi: 10.5383/ijtee.19.01.005.

[7] U. Ali, M. Islam, and I. Janajreh, "Parametric Optimization for Thermoacoustic Refrigerator Driven by Thermoacoustic Engine," in *9th International Conference on Fluid Flow, Heat and Mass Transfer (FFHMT'22)*, 2022, p. 10.11159/ffhmt22.209.

[8] U. Ali, Y. Al Masalmeh, S. Abedrabbo, M. Islam, and I. Janajreh, "Numerical Simulation and Experimental Validation of Thermoacoustic Engine," in *ASME 2022 16th International Conference on Energy Sustainability*, Philadelphia, Pennsylvania, USA: American Society of Mechanical Engineers, Jul. 2022, p. V001T10A007. doi: 10.1115/ES2022-85821.

[9] Y. Al Masalmeh, U. Ali, M. Islam, and I. Janajreh, "Effect of Stack Position and Stack Length on the Performance of Thermoacoustic Engine," in *9th International Conference on Fluid Flow, Heat and Mass Transfer (FFHMT'22)*, 2022, p. 10.11159/ffhmt22.208.

[10] N. M. Hariharan, P. Sivashanmugam, and S. Kasthurirengan, "Influence of stack geometry and resonator length on the performance of thermoacoustic engine," *Applied Acoustics*, vol. 73, no. 10, pp. 1052–1058, Oct. 2012, doi: 10.1016/j.apacoust.2012.05.003.

[11] G. Yu, W. Dai, and E. Luo, "CFD simulation of a 300Hz thermoacoustic standing wave engine," *Cryogenics*, vol. 50, no. 9, pp. 615–622, Sep. 2010, doi: 10.1016/j.cryogenics.2010.02.011.

[12] S. Elshabrawy, M. Hussain, and I. Janajreh, "Thermo-acoustic Engine Pressure Wave: Analysis of Working Fluid Effect," Volume 5: Innovative Solutions for Energy Transitions: Part IV, preprint, Mar. 2020. doi: 10.46855/energy-proceedings-4407.

[13] S. Dong, G. Shen, M. Xu, S. Zhang, and L. An, "The effect of working fluid on the performance of a large-scale thermoacoustic Stirling engine," *Energy*, vol. 181, pp. 378–386, Aug. 2019, doi: 10.1016/j.energy.2019.05.142.

[14] H. Zhang, S. Abedrabbo, and I. Janajreh, "Numerical simulation of the travelling wave thermo-acoustic engine and parametric sensitivity," presented at the 15th International Conference on Heat Transfer, Fluid Mechanics and Thermodynamics, 2021.